

Scientific paper

Biosorption of Hexavalent Chromium Metal Ions by *Lentinula Edodes* Biomass: Kinetic, Isothermal, and Thermodynamic Parameters

Aslı Göçenoğlu Sarıkaya*

* Bursa Uludağ University, Faculty of Art and Science, Department of Chemistry, Görükle Campus, Turkey,

* Corresponding author: E-mail: agocenoglu@uludag.edu.tr
+90 224 294 28 67

Received: 09-23-2020

Abstract

Lentinula edodes was investigated as a biosorbent for hexavalent chromium biosorption in this study. To examine the optimum conditions of biosorption, the pH of the hexavalent chromium solution, biosorbent dosage, temperature, contact time, and initial hexavalent chromium concentration were identified. Further, to clarify the biosorption mechanism process, the isothermal, kinetic, and thermodynamic parameters were determined. The functional groups and surface morphology of the biosorbent were identified using Fourier transform infrared spectrometry and scanning electron microscopy in the absence and presence of hexavalent chromium, respectively. Based on the results, the maximum biosorption capacity was determined as 194.57 mg g⁻¹ under acidic conditions at 45 °C. From the kinetics studies, the biosorption process was observed to follow the Freundlich isotherm and pseudo-second-order kinetic models well. Thus, *L. edodes* as a biosorbent has potential usage for wastewater treatment owing to its effective biosorption capacity.

Keywords: Biosorption, fungal biosorbent, hexavalent chromium, *Lentinula edodes*.

1. Introduction

Pollution by heavy metal impurities is one of the major problems of increasing industrial development.^{1,2} Chromium is one of the common pollutants in nature and exists in different oxidation states (-2 to +6) in the environment; however, trivalent chromium (Cr³⁺) and hexavalent chromium (Cr⁶⁺) forms tend to be the most available and stable oxidation states in water.³ The hexavalent form of chromium is more toxic than the trivalent form and is known as a carcinogenic that causes liver damage, congestion in the lungs, changes to the genetic code, and skin irritation.⁴⁻⁶ The most common sources of hexavalent chromium wastes are industrial sectors such as textiles, metal finishing, leather tanning, electroplating, cement, and steel.^{7,8}

The traditional processes used to remove hexavalent chromium are electrochemical reduction, solvent extraction, electro dialysis, ion exchange, reverse osmosis, and chemical precipitation. Owing to disadvantages such as high cost and increased time consumption of these methods, new procedures have been developed. Biosorption is one of the alternative methods for wastewater treatment and is widely used in batch and continuous studies because

of its advantages such as low cost, reusability, and easy operation, which are attractive benefits.^{9,10} Shells,¹¹ leaves,¹² fungi,⁹ bacteria,¹³ and yeast¹⁴ have been previously reported as biosorbents for hexavalent chromium biosorption.

Lentinula edodes ranks second in the global mushroom market and is commonly known as ‘shiitake mushroom’¹⁵ it is- the most popular edible mushroom in Japan and China-, and its nutritional components enable *L. edodes* to be used as traditional medicinal mushrooms in eastern Asia. It grows in the deciduous forests of Asia under warm and humid climatic conditions. The goal of this study is to verify removal of hexavalent chromium from water using *L. edodes* as a biosorbent. The effects of different parameters on the biosorption process, reusability of the biosorbent, and some physicochemical parameters are optimized in this study.

2. Materials and Methods

2.1. *L. edodes* Biosorbent Preparation

L. edodes was obtained from a commercial market in Izmir (Turkey), washed twice with deionized water, and

dehydrated at 30 °C. The dried fungus was then crushed with a grinder after cutting into small pieces. The biosorbent powder (90–120 µm size) was subsequently stored in a glass jar for biosorption studies.

2. 2. Batch Biosorption Experiments

The stock solution of hexavalent chromium (1000 mg L⁻¹) was prepared by dissolving K₂Cr₂O₇ (Sigma-Aldrich) in pure water and diluting in the range of 10–1000 mg L⁻¹. Approximately 0.01 g of the *L. edodes* biosorbent was used in the biosorption processes with 25 mL total volume of known hexavalent chromium solutions. To obtain the optimum pH in the range of 2–6, the solution was maintained using 0.1 mol L⁻¹ NaOH and 0.1 mol L⁻¹ HCl. The impact of temperature was examined via experiments performed at 4, 25, and 45 °C. To optimize the contact time, the biosorption process was conducted for 10–180 min. The biosorbent was removed from the solution before analyzing the remaining hexavalent chromium solution via centrifugation for 10 min at 5000 rpm, and the supernatant was analyzed according to the 1,5-diphenylcarbazide spectrophotometric method at 540 nm (Perkin Elmer Lambda 35 UV/Vis Spectrometer).

The hexavalent chromium concentration at equilibrium can be determined according to Eq. 1 as follows:

$$q_e = \frac{(C_0 - C_e)}{m} V \quad (1)$$

where q_e is the amount of absorbed hexavalent chromium ions (mg g⁻¹), C_0 and C_e are the initial and final concentrations of hexavalent chromium (mg L⁻¹), V is the total solution volume (mL), and m is the mass of the biosorbent (g).

Desorption percentages were calculated with 0.1 mol L⁻¹ HNO₃ and 0.1 mol L⁻¹ HCl using the following equation:

$$\% \text{ Desorption} = \frac{C_{des}}{C_{ads}} \times 100 \quad (2)$$

where C_{des} is the amount of hexavalent chromium ions desorbed on the desorption medium and C_{ads} is the amount of hexavalent chromium ions adsorbed onto the biosorbent. The adsorbed biosorbents were shaken at 200 rpm on a magnetic shaker at 25 °C for 24 h.

2. 3. Characterization of Biomass

Fourier transform infrared (FTIR) spectroscopy (Perkin Elmer Spectrum BX FTIR System) and scanning electron microscopy (SEM, ZEISS EVO 40) were used to identify the binding sites and functional groups on the fungal biosorbent surface as well as the surface morphology of the biosorbent in the absence and presence of hexavalent chromium, respectively.

3. Results and Discussion

3. 1. Effects of pH

The pH of an aqueous solution is a crucial factor for the biosorption process and affects the ion sorption efficiency. The charges of the functional groups of the biosorbent and distribution of the hexavalent chromium species are affected by changes in the solution pH. Therefore, the biosorption and reduction processes have different affinities.¹⁶ The maximum biosorption capacity (q_e) of hexavalent chromium on the *L. edodes* biosorbent was determined as 6.12 mg g⁻¹ at a pH of 2.0 (Figure 1).

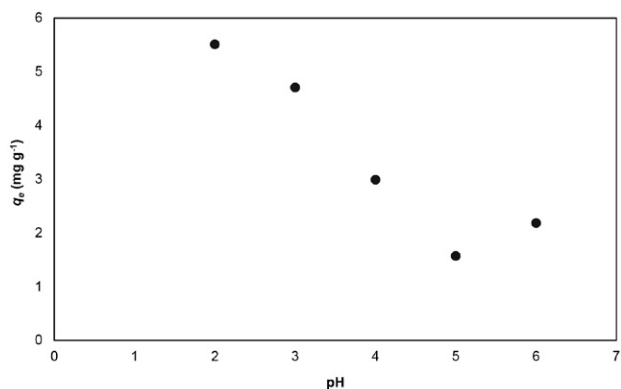


Figure 1. Effect of pH on hexavalent chromium biosorption capacity (q_e) onto *L. edodes* biosorbent.

The experiments were performed for 120 min at 25 °C with 10 mg L⁻¹ as the initial hexavalent chromium concentration, hence, the suitable pH was chosen as 2.0 for biosorption. Generally, in aqueous hexavalent chromium solutions, HCrO₄⁻, Cr₂O₇²⁻, CrO₄²⁻, and H₂CrO₄ are the dominant species.¹⁷ Under acidic condition (pH ≤ 4.0) HCrO₄⁻, Cr₂O₇²⁻, and H₂CrO₄ are the main forms of hexavalent chromium. HCrO₄⁻ is the dominant form of hexavalent chromium at a pH of 2.0.¹⁸ Owing to protonation of the amino functional groups, the cell surface become positively charged, hence, the acid chromate can perfectly interact with the protonated biomass surface.^{3,19}

3. 2. Effects of Biosorbent Dosage

To examine the effects of biosorbent dosage on hexavalent chromium biosorption, different amounts of the biosorbent were tested in the range of 0.025–0.200 g. Approximately 100 mg mL⁻¹ of the initial hexavalent chromium concentration and 25 mL of total volume of the ion solutions were used at 25 °C. As the biosorbent dosage increased from 0.025 g to 0.200 g, the q_e value decreased from 24.46 mg g⁻¹ to 3.94 mg g⁻¹ (Figure 2). As the total amount of hexavalent chromium biosorbed on the biosorbent increases, the q_e per unit of biomass reduces because of the fixed concentration.²⁰

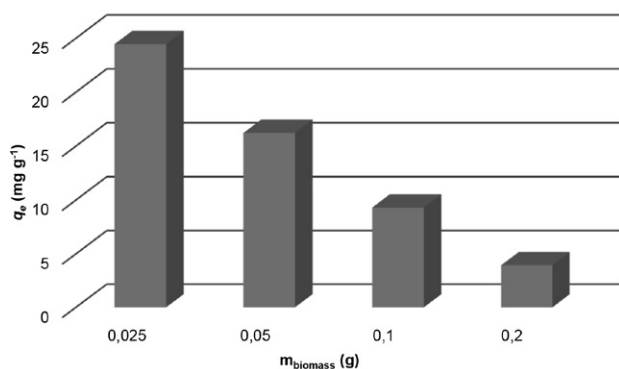


Figure 2. Effect of biosorbent dosage on hexavalent chromium biosorption capacity (q_e) onto the *L. edodes* biosorbent.

3. 3. Effects of Initial Concentration of Hexavalent Chromium and Contact Time

To understand the effects of initial concentration of the hexavalent chromium, 10–1000 mg L⁻¹ initial concentrations were tested for the 25 mL total solution volume and 0.025 g of the biosorbent. The q_e increased from 4.56 to 110.96 mg g⁻¹ with increase in the initial hexavalent chromium concentration from 10 to 1000 mg L⁻¹ at 25 °C. To identify the impact of temperature on the biosorption process, three different temperature values of 4, 25, and 45 °C were studied at both initial concentrations. The total volume of the hexavalent chromium solution and amount of biosorbent were 25 mL and 0.01 g, respectively. As seen in Figure 3, when the temperature increases from 4 to 45 °C, the q_e increases from 1.33 to 11.26 mg g⁻¹ at 10 mg L⁻¹ initial hexavalent chromium concentration. Figure 3 also depicts that the q_e values at 4, 25, and 45 °C are 87.67, 110.96 and 194.57 mg g⁻¹, respectively.

To examine the effects of contact time, about 0.025 g of the biosorbent in 25 mL of the total solution volume with 100 mg L⁻¹ hexavalent chromium solution was tested at 4, 25, and 45 °C for 10–180 min. At 4 °C, q_e increased

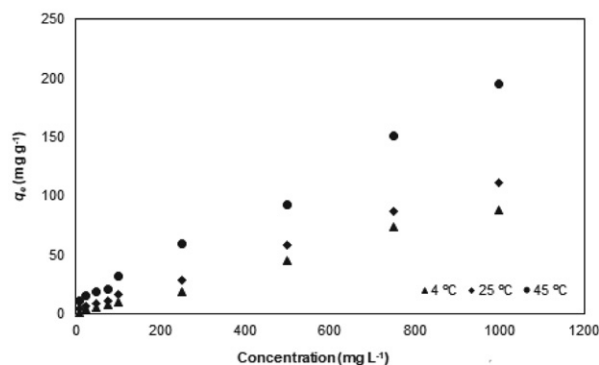


Figure 3. Effect of initial concentration of hexavalent chromium on its biosorption capacity (q_e) onto the *L. edodes* biosorbent.

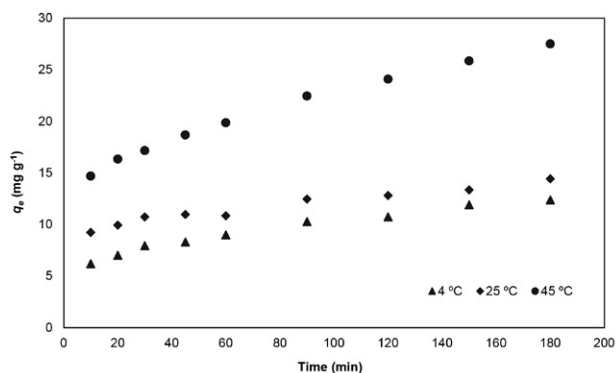


Figure 4. Effect of contact time on hexavalent chromium biosorption capacity (q_e) onto the *L. edodes* biosorbent.

from 6.19 to 12.38 mg g⁻¹, with temperature increase from 25 to 45 °C, q_e increased from 14.42 to 27.48 mg g⁻¹. These results are illustrated in Figure 4.

3. 4. Biosorption Isotherms

To identify the interactions between the sorbate (liquid or gas) and sorbent, sorption isotherms were used. The Langmuir, Freundlich, and Sips isotherm models were investigated in this study. In the Langmuir isotherm model, the sorbate molecules interact with the sorbent molecules to form a monolayer, uniform and homogenous surface. In this model, all sorption sites are unique and morphologically homogeneous. The Langmuir equation can be expressed as follows:

$$\frac{C_e}{q_e} = \frac{1}{Q_L K_L} + \frac{C_e}{Q_L} \quad (3)$$

where K_L is the Langmuir constant (L mg⁻¹), C_e is the hexavalent chromium concentration under equilibrium (mg L⁻¹), q_e is the amount of biosorbed hexavalent chromium (mg g⁻¹) and Q_L is the maximum Langmuir monolayer coverage capacity (L mg⁻¹).²¹

The Freundlich isotherm model is suitable for heterogeneous surfaces and a reversible sorption process for multilayer sorbents. The Freundlich isotherm equality is given as follows:

$$\ln q_e = \ln K_F + \frac{1}{n} \ln C_e \quad (4)$$

Here, K_F represents the Freundlich isotherm and n is the biosorption intensity. The value of $1/n$ characterizes the feasibility of the isotherm.²² To investigate the applicability of the isotherm, a linear graph of $\ln q_e$ versus $\ln C_e$ was plotted, and the K_F and n values were calculated from the intercept and slope of the plot, respectively.²³

The Sips isotherm equality is given as follows:

$$\frac{1}{q_e} = \frac{1}{Q_{\max} K_S} \left(\frac{1}{C_e} \right)^{1/n} + \frac{1}{Q_{\max}} \quad (5)$$

where, Q_{max} is the maximum biosorption capacity (mg g^{-1}) and K_S is the Sips constant (L mg^{-1}).

The calculated data are given in Table 1. As seen, the *L. edodes* fits better with the Freundlich model than the Langmuir or Sips models. The K_F values were determined as 0.69, 0.20, and 0.19 L mg^{-1} at 4, 25, and 45 °C, respectively. The $1/n$ value gives the heterogeneity of the surface,²⁴ so the n values were calculated as 0.90, 0.75, and 0.65 at 4, 25, and 45 °C, respectively.

$\text{g}^{-1} \text{min}^{-1/2}$), and $t^{1/2}$ is the half-life time (s). Plots of the biosorbate uptake q_t versus $t^{1/2}$ show a linear relationship when the IPD is rate limited.

The RSO model is expressed as follows:²⁸

$$\frac{1}{q_t} = \frac{1}{k_R q_e t} + \frac{1}{q_e} \quad (12)$$

Here, k_R is the RSO rate constant (min^{-1}), q_e and q_t are the amounts of biosorbed hexavalent chromium at

Table 1. Biosorption isotherm constants for hexavalent chromium biosorption onto the *L. edodes* biosorbent.

T (K)	Langmuir Isotherm Constants			Freundlich Isotherm Constants			Sips Isotherm Constants		
	$K_L \times 10^2$ (L mg^{-1})	Q_L (mg g^{-1})	R^2	K_F (L mg^{-1})	N	R^2	$K_S \times 10^2$ (L mg^{-1})	Q_{max} (mg g^{-1})	R^2
277	0.35	39.06	0.88	0.69	0.90	0.99	0.30	36.10	0.99
298	3.43	14.68	0.95	0.20	0.75	0.97	2.84	11.55	0.83
318	7.41	24.33	0.99	0.19	0.65	0.96	3.72	19.84	0.95

3. 5. Biosorption Kinetics

Kinetic analysis is important to clarify the transport mechanisms of biosorption, which have to be identified. Langergeren's first order (LFO), pseudo-second order (PSO), intraparticle diffusion (IPD), and Ritchie's second-order (RSO) kinetic models were thus calculated to identify the biosorption processes.

The LFO and PSO models are expressed as follows:^{25,26}

$$\ln(q_e - q_t) = \ln q_e - k_1 t \quad (9)$$

$$\frac{t}{q_t} = \frac{1}{k_2 q_e^2} + \frac{t}{q_e} \quad (10)$$

Here, q_e is the amount of biosorbed hexavalent chromium at equilibrium time (mg g^{-1}), q_t is the amount of biosorbed hexavalent chromium at time t (min), and k_1 (min^{-1}) and k_2 (mol kg min^{-1}) are the LFO and PSO rate constants, respectively.

The IPD model represents the rate-limiting steps and is given as follows:²⁷

$$q_t = k_{id} t^{1/2} \quad (11)$$

where q_t is the amount of biosorbed hexavalent chromium at time t (mol kg^{-1}), k_{id} is the IPD rate constant (mg

equilibrium time (mg g^{-1}) and at time t (min), respectively. In this model, the number of surface sites, n , are bounded by each biosorbate. The kinetic models are summarized at Table 2. According to the calculated values, the PSO kinetic model is suitable for the biosorption process. The R^2 values were 0.99 for all three temperatures (4, 25, and 45 °C), and the calculated q_e values, which are similar to the experimental q_e (Eq. 1) values, are 1.63, 4.27, and 12.05 mg g^{-1} , respectively. Comparative results of the biosorption of Cr(VI) by various sorbents are given in Table 3.

3. 6. Biosorption Thermodynamics

The van't Hoff equation was used to calculate the thermodynamic parameters at different temperatures. The free energy change (ΔG°), entropy change (ΔS°), and enthalpy change (ΔH°) values were determined as follows:

$$\ln K_L = -\frac{\Delta H^\circ}{RT} + \frac{\Delta S^\circ}{R} \quad (13)$$

$$\Delta G^\circ = \Delta H^\circ - T\Delta S^\circ \quad (14)$$

where T represents the absolute temperature (K), R is the universal gas constant ($8.314 \text{ J mol}^{-1} \text{ K}^{-1}$), and K_L is the Langmuir equilibrium constant.

Table 2. Biosorption kinetic models and parameters for hexavalent chromium biosorption onto the *L. edodes* biosorbent.

T (K)	LFO				PSO			IPD			RSO		
	$q_e \text{ exp}$ (mg g^{-1})	$k_1 \times 10^2$ (min^{-1})	q_e (mg g^{-1})	R^2	$k_2 \times 10^2$ (mol kg min^{-1})	q_e (mg g^{-1})	R^2	k_{id} ($\text{mg g}^{-1} \text{ min}^{-1/2}$)	R^2	k_R (min^{-1})	q_{eq} (mg g^{-1})	R^2	
277	1.32	1.60	2.08	0.93	7.49	1.63	0.99	0.60	0.99	4.37	6.02	0.85	
298	4.56	1.72	2.07	0.66	7.01	4.27	0.99	0.42	0.88	8.06	4.23	0.55	
318	11.26	1.38	2.76	0.98	3.42	12.05	0.99	1.25	0.99	10.49	12.50	0.79	

Table 3. Biosorption of Cr(VI) by different sorbents.

Sorbent	Sorption capacity	pH	Time	T (K)	Isotherm model	Kinetic model	Reference
<i>Arthrobacter viscosus</i>	14.4 mg/g	2	144 h	299	Langmuir	–	29
<i>Spirulina</i> sp.	59.57 mg/g	5	60 min	298	Langmuir and Freundlich	PSO	30
<i>Agaricus campestris</i>	56.21 mg/g	2	60 min	318	Langmuir	PSO	9
Multi-shell hollow micro-meso-macroporous silica	257.67 mg/g	4	90 min	293	Langmuir	–	31
Activated carbon	54.8 mg/g	3.5	72 h	333	Langmuir	PSO	32
Cellulose hydrogel coating with Fe ⁰	98.2 %	5	4 h	313	–	LFO	33
Sugarcane bagasse	87 %	6.7	100 min	319	Redlich-Peterson and Temkin	LFO	34
<i>Lentinula edodes</i>	194,57 mg g ⁻¹	2	3 ure	318,	Freundlich	PSO	This study

Positive or negative values of ΔG° indicate the spontaneity or non-spontaneity of the biosorption process, ΔH° supplies information about the process and whether it is exothermic or endothermic.³⁵ Finally, another thermodynamic parameter, ΔS° , gives information about the randomness of the biosorption process. The thermodynamic parameters were calculated using Eq. 14, and these data are given in Table 4. It is observed that biosorption is an exothermic process ($\Delta H^\circ = -4.587 \text{ kJ mol}^{-1}$) and that the randomness decreases during the process ($\Delta S^\circ = -0.738 \text{ J mol}^{-1} \text{ K}^{-1}$). The calculated ΔG° values were 3.61, 3.36, and 3.14 kJ mol^{-1} at 4, 25, and 45 °C, respectively. These results indicate that ΔG° decreases with increasing temperature and that the biosorption process is suitable for high temperatures.

Table 4. Thermodynamic parameters for hexavalent chromium biosorption onto the *L. edodes* biosorbent.

$\Delta H^\circ (\text{kJ mol}^{-1})$	-4.587		
$\Delta S^\circ (\text{J mol}^{-1} \text{ K}^{-1})$	-0.738		
$\Delta G^\circ (\text{kJ mol}^{-1})$	277 K	298 K	318 K
	3.61	3.36	3.14

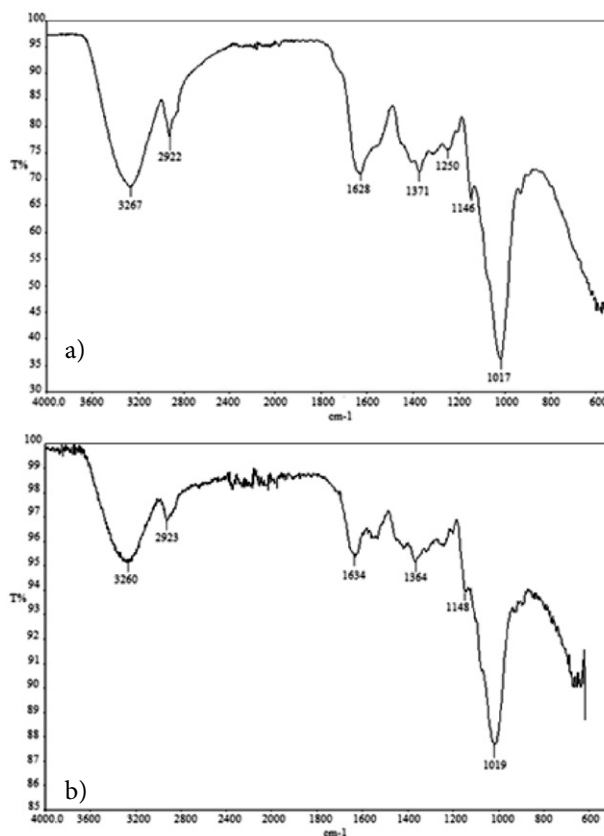
3. 7. Desorption and Reusability of the Biosorbent

Approximately 0.1 mol L⁻¹ HCl and 0.1 mol L⁻¹ of HNO₃ were used as the desorption agents, and based on the results, the 0.1 mol L⁻¹ concentration of HNO₃ (96.37%) was more effective than 0.1 mol L⁻¹ of HCl (35.89%). To determine the reusability of the *L. edodes* as a biosorbent, the biosorption–desorption cycles were repeated five times, during which the biosorption capacity decreased by 7%.

3. 8. Characterization of the Biosorbent

The effective functional groups of the *L. edodes* biosorbent for hexavalent chromium biosorption were ex-

amined using FTIR spectroscopy. The FTIR spectra of the biosorbent before and after biosorption in the range of 4000–600 cm⁻¹ are given in Figure 5. The strong and broad bands at 3267 and 3260 cm⁻¹ are attributed to the -OH and -NH groups before and after biosorption, respectively. The peak at 2922 cm⁻¹ are attributed to C-H stretching, and the peaks observed at 1628–1634 cm⁻¹ correspond to carboxylate functional groups and carboxyl groups of the biosorbent. Stretching of the -COO group is represented at 1371–1364 cm⁻¹, and the peaks at 1017–1019 cm⁻¹ are assigned to N-H or C-O band absorption.

Figure 5. FTIR spectra of the *L. edodes* biosorbent (a) before and (b) after biosorption of hexavalent chromium.

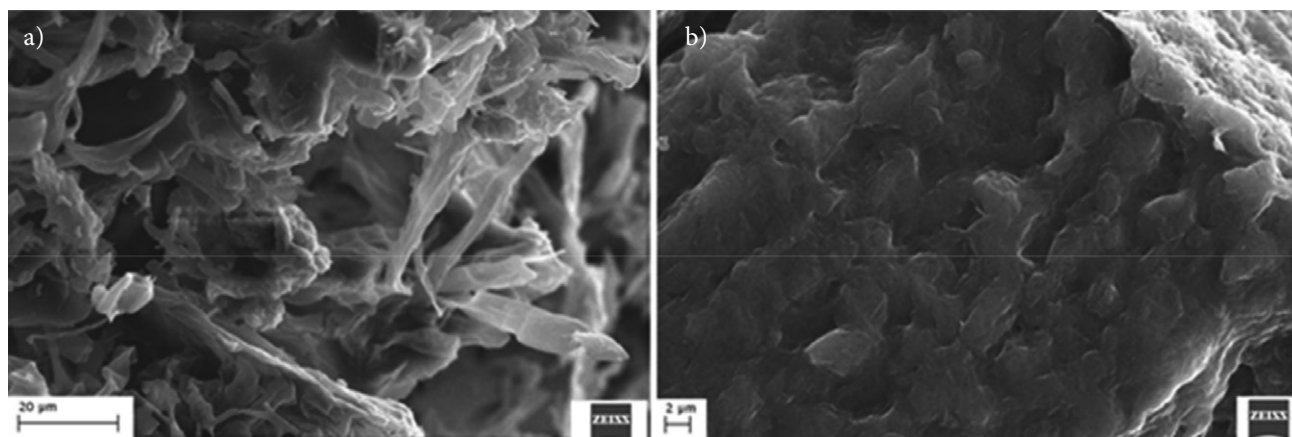


Figure 6. SEM images of the *L. edodes* biosorbent (a) before and (b) after biosorption of hexavalent chromium.

To identify the surface morphology of the biosorbent SEM was used. As seen in Figure 6, the surface of the biomass has some heterogeneity and becomes smoother after biosorption owing to binding of the hexavalent chromium ions to the functional sites of the biosorbent.

4. Conclusion

The main aim of this study was to examine the viability of *L. edodes* as a biosorbent for hexavalent chromium biosorption. In this assessment, the optimum biosorption parameters such as pH, temperature, biosorbent dosage, and contact time, were determined. The optimum process parameters were detected as pH of 2.0, total biosorbent dosage of 0.025 g, and maximum biosorption capacity of 194.57 mg g⁻¹ during 3 h of biosorption at 45 °C. The obtained data were applied to certain physicochemical parameters, such as isotherm, thermodynamic, and kinetic models, to identify the biosorption process. The Freundlich isotherm and PSO kinetic models were found to be suitable for the biosorption process and observed to fit well with the experimental data. The standard enthalpy and standard entropy were calculated as -4.587 kJ mol⁻¹ and -0.738 J mol⁻¹ K⁻¹, respectively. In addition, the *L. edodes* biosorbent was determined to be an effective and a renewable biomaterial that was suitable for hexavalent chromium biosorption from aqueous solutions, this biosorbent showed high sorption capacity for treatment of wastewater contaminated with hexavalent chromium.

5. References

1. J. R. M. B. Smily, P. A. Sumithra, *HAYATI J. Biosci.* **2017**, *24*(2), 65–71. DOI:10.1016/j.hjb.2017.08.005
2. J. Wang, Q. Xie, A. Li, X. Liu, F. Yu, J. Ji, *Water Sci. Technol.* **2020**, *81*(6), 1114–1129. DOI:10.2166/wst.2020.167
3. N. K. Mondal, A. Samanta, S. Dutta, S. Chatteroj, *J. Genet. Eng. Biotechnol.* **2017**, *15*(1), 151–160. DOI:10.1016/j.jgeb.2017.01.006
4. J. J. Pan, J. Jiang, R. K. Xu, *Chemosphere*, **2014**, *101*, 71–76. DOI:10.1016/j.chemosphere.2013.12.026
5. Y. Li, Y. Wei, S. Huang, X. Liu, Z. Jin, M. Zhang, J. Qu, Y. Jin, *J. Mol. Liq.* **2018**, *269*, 824–832. DOI:10.1016/j.molliq.2018.08.060
6. Z. Shi, S. Peng, X. Lin, Y. Liang, S. -Z. Lee, H. E. Allen, *Environ. Sci. Process. Impacts.* **2020**, *22*, 95–104. DOI:10.1039/C9EM00477G
7. E. Nakkeeran, C. Patra, T. Shahnaz, S. Rangabhashiyam, N. Selvaraju, *Bioresour. Technol. Reports.* **2018**, *3*, 256–260. DOI:10.1016/j.biteb.2018.09.001
8. R. Xiao, J. J. Wang, R. Li, J. Park, Y. Meng, B. Zhou, S. Pensky, Z. Zhang, *Chemosphere.*, **2018**, *208*, 408–416. DOI:10.1016/j.chemosphere.2018.05.175
9. A. Göçenoğlu Sarıkaya, *Environ. Technol.* **2021**, *42*(1), 72–80. DOI:10.1080/09593330.2019.1620867
10. S. H. Abbas, Y. M. Younis, M. K. Hussain, F. H. Kamar, G. Nechifor, B. Pasca, *Rev. Chim.* **2020**, *71*(1), 1–12. DOI:10.37358/RC.20.1.7804
11. C. Patra, T. Shahnaz, S. Subbiah, S. Narayanasamy, *Environ. Sci. Pollut. Res.* **2020**, *27*, 14836–14851. DOI:10.1007/s11356-020-07979-y
12. A. K. Prajapati, S. Das, M. K. Mondal, *J. Mol. Liq.* **2020**, *307*, 112956. DOI:10.1016/j.molliq.2020.112956
13. V. Kalola, C. Desai, *Environ. Sci. Pollut. Res.* **2019**. DOI:10.1007/s11356-019-05942-0
14. A. De Rossi, M. R. Rigon, M. Zapparoli, R. D. Braido, L. M. Colla, G. L. Dotto, J. S. Piccin, *Environ. Sci. Pollut. Res.* **2018**, *25*(19), 19179–19186. DOI:10.1007/s11356-018-2377-4
15. P. S. Bisen, R. K. Baghel, B. S. Sanodiya, G. S. Thakur, G. B. Prasad, *Curr. Med. Chem.* **2010**, *17*(22), 2419–2430. DOI:10.2174/092986710791698495
16. T. Chen, Z. Zhou, S. Xu, H. Wang, W. Lu, *Bioresour. Technol.* **2015**, *190*, 388–394. DOI:10.1016/j.biortech.2015.04.115
17. P. Miretzky, A. Cirelli, *J. Hazard. Mater.* **2010**, *180*(1–3), 1–19. DOI:10.1016/j.jhazmat.2010.04.060
18. S. Sugashini, K. M. M. S. Begum, *Clean. Technol. Environ. Policy.* **2013**, *15*, 293–302. DOI:10.1007/s10098-012-0512-3
19. Z. Aksu, U. Açikel, E. Kabasakal, S. Tezer, *Water Res.* **2002**,

- 36(12), 3063–3073. DOI:10.1016/S0043-1354(01)00530-9
20. Z. K. Wang, C. L. Ye, X. Y. Wang, J. Li, *Appl. Surf. Sci.* **2013**, 287, 232–241. DOI:10.1016/j.apsusc.2013.09.133
21. I. Langmuir, *J. Am. Chem. Soc.* **1918**, 40(9), 1361–143. DOI:10.1021/ja02242a004
22. E. Radu, E. E. Oprescu, C. E. Enascuta, C. Calin, R. Stoica, G. V. Scaeteanu, G. Vasilevici, L. Capra, G. Ivan, A. C. Ion, *Rev. Chim.* **2018**, 69(1), 191–195. DOI:10.37358/RC.18.1.6072
23. H. Freundlich, *J. Phys. Chem. A.* **1906**, 57, 385–471.
24. Y. Özüdoğru, M. Merdivan, *Trak. Univ. J. Nat. Sci.* **2017**, 18(2), 81–87. DOI:10.23902/trkjnat.300344
25. S. Lagergren, *Sven. Vetenskapsakad Handlingar*, **1898**, 24, 1–39.
26. S. K. Srivastava, V. K. Gupta, S. Anurpam, D. Mohan, *Indian J. Chem.* **1995**, 34A, 342–350.
27. T. Furusawa, J. M. Smith, *AIChE Journal*, **1974**, 20, 88. DOI:10.1002/aic.690200111
28. A. G. Ritchie, *J. Chem. Soc. Faraday Trans.* **1977**, 73, 1650. DOI:10.1039/f19777301650
29. R. M. Hlihor, H. Figueiredo, T. Tavares, M. Gavrilescu, *Process. Saf. Environ.* **2017**, 108, 44–56. DOI:10.1016/j.psep.2016.06.016
30. H. Rezaei, *Arab. J. Chem.* **2016**, 9, 846–853. DOI:10.1016/j.arabjc.2013.11.008
31. R. Soltani, A. Marjani, R. Soltani, S. Shirazian, *Sci. Rep.* **2020**, 10, 9788. DOI:10.1038/s41598-020-66540-6
32. Y. Wang, C. Peng, E. Padilla-Ortega, A. Robledo-Cabrera, A. Lopez-Valdivieso, *J. Environ. Chem. Eng.* **2020**, 8(4), 104031. DOI:10.1016/j.jece.2020.104031
33. Y. Wang, L. Yu, R. Wang, Y. Wang, X Zhang, *Sci. Total Environ.* **2020**, 726, 138625. DOI:10.1016/j.scitotenv.2020.138625
34. R. R. Karri, J. N. Sahu, B. C. Meikap, *Industrial Crops and Products*, **2020**, 143, 111927. DOI:10.1016/j.indcrop.2019.111927
35. R. M. Senin, I. Ion, O. Oprea, R. Stoica, R. Ganea, A. C. Ion, *Rev. Chim.* **2018**, 69(5), 1233–1239. DOI:10.37358/RC.18.5.6297

Povzetek

Namen študije je bil preučitev sposobnosti adsorpcije kroma (VI) z glivo šitake (*Lentinula edodes*). Da bi določili optimalne pogoje smo spreminjali pH vrednost raztopine kroma (VI), količino šitake, temperaturo, kontaktni čas in koncentracijo kroma (VI). Adsorpcijski mehanizem smo opisali z izotermičnimi, kinetičnimi in termodinamskimi parametri. Funkcionalne skupine in morfologijo površine glive smo analizirali s FTIR in SEM v odsotnosti in prisotnosti kroma (VI). Maksimalna adsorpcijska kapaciteta je znašala 194.57 mg g⁻¹, pod kislimi pogoji pri temperaturi 45 °C. Na osnovi kinetičnih študij smo zaključili, da lahko ravnotežje opišemo s Freundlichovo izotermo, adsorpcijo pa s kinetičnim modelom psevdoprvega reda. Visoka adsorpcijska sposobnost *L. edodes* kaže potencial njene uporabe za čiščenje odpadnih vod.



Except when otherwise noted, articles in this journal are published under the terms and conditions of the Creative Commons Attribution 4.0 International License